The Product of the Spindle Formation Gene *sad1*$^+$ Associates with the Fission Yeast Spindle Pole Body and Is Essential for Viability

Iain Hagan and Mitsuhiro Yanagida

Department of Biophysics, Faculty of Science, Kyoto University, Kitashirakawa, Sakyo-ku, Kyoto 606, Japan

Abstract. Spindle formation in fission yeast occurs by the interdigitation of two microtubule arrays extending from duplicated spindle pole bodies which span the nuclear membrane. By screening a bank of temperature-sensitive mutants by anti-tubulin immunofluorescence microscopy, we previously identified the *sad1.1* mutation (Hagan, I., and M. Yanagida. 1990. *Nature (Lond.).* 347:563–566). Here we describe the isolation and characterization of the *sad1*$^+$ gene. We show that the *sad1.1* mutation affected both spindle formation and function. The *sad1*$^+$ gene is a novel essential gene that encodes a protein with a predicted molecular mass of 58 kD. Deletion of the gene was lethal resulting in identical phenotypes to the *sad1.1* mutation. Sequence analysis predicted a potential membrane-spanning domain and an acidic amino terminus. Sad1 protein migrated as two bands of 82 and 84 kD on SDS-PAGE, considerably slower than its predicted mobility, and was exclusively associated with the spindle pole body (SPB) throughout the mitotic and meiotic cycles. Microtubule integrity was not required for Sad1 association with the SPB. Upon the differentiation of the SPB in metaphase of meiosis II, Sad1-staining patterns similarly changed from a dot to a crescent supporting an integral role in SPB function. Moderate overexpression of Sad1 led to association with the nuclear periphery. As Sad1 was not detected in the cytoplasmic microtubule-organizing centers activated at the end of anaphase or kinetochores, we suggest that Sad1 is not a general component of microtubule-interacting structures per se, but is an essential mitotic component that associates with the SPB but is not required for microtubule nucleation. Sad1 may play a role in SPB structure, such as maintaining a functional interface with the nuclear membrane or in providing an anchor for the attachment of microtubule motor proteins.

THE accurate duplication and segregation of genetic information from a parent cell into two daughter cells is a fundamental property of biological systems. Most eukaryotic cells accomplish this complex task by temporally separating different events into a discrete number of interdependent steps. Thus DNA synthesis usually occurs early in the cell cycle and is separated from chromosome segregation by a gap period. Considerable progress has been made in understanding the regulation of these events, in particular the transition of the rate limiting step of commitment to mitosis through the activation of a multicomponent kinase called M-phase Promoting Factor (MPF)[1] (Nurse, 1990). Despite this increased understanding of the controlling network, our knowledge of the underlying basis of the subsequent chromosome condensation and spindle function remains limited. The morphological aspects of spindle behavior have been well established, but the identities of many spindle components and their specific molecular functions in the spindle remain obscure (Rieder and Salmon, 1994).

When spindle formation is initiated by the activation of MPF, the interphase cytoplasmic microtubule network undergoes a radical change. This involves severing existing microtubules, the alteration of the dynamics of microtubules radiating from, and the combined activation and splitting of the principle microtubule-organizing center (MTOC—the centrosome in higher eukaryotes) (Ault and Rieder, 1994; Belmont et al., 1990; Buendia et al., 1992; Gotoh et al., 1990; Shiina et al., 1992; Vale, 1991; McNally and Vale, 1993; Verde et al., 1992). These steps of MTOC activation are considered to be MPF dependent (Centonze and Borisy, 1990; Masuda et al., 1992; Buendia et al., 1992; Verde et al., 1990, 1992).

Many recent advances in the identification of spindle components has come from genetic analyses of mutants that affect microtubule or spindle function. This has been particularly apparent with the recent identification of many putative mitotic microtubule motors on the basis of combined DNA sequence homology and mutant phenotype (Goldstein, 1993).

Please address all correspondence to Dr. Iain Hagan, 2.205 School of Biological Sciences, University of Manchester, Stopford Building, Oxford Road, Manchester, M13 9PT, United Kingdom. Tel.: 44 61 275 5512. Fax: 44 61 275 5082.

1. *Abbreviations used in this paper*: MPF, M-phase Promoting Factor; MTOC, microtubule-organizing centre; *sad*, spindle architecture disrupted; SPB, spindle pole body.

We have been using the fission yeast *Schizosaccharomyces pombe* as a model system in which to use such a genetic approach towards the identification of spindle components (Yanagida, 1989; Samejima et al., 1993). Fission yeast is well suited for this task as its microtubule cytoskeleton is typically eukaryotic with exclusively cytoplasmic microtubules during interphase which depolymerize as a spindle is formed upon mitotic commitment (Hagan and Hyams, 1988). Spindle microtubules assemble from two spindle pole bodies (SPBs) that are probably activated by MPF-dependent phosphorylation (Masuda et al., 1992). Spindle microtubules are polar and a typical spindle forms by interdigitation of two polarized arrays (McCully and Robinow, 1971; Tanaka and Kanbe, 1986; Masuda et al., 1990; Ding et al., 1993). At the end of an extended anaphase B the spindle breaks down, the SPBs are turned off, and interphase microtubules assemble from two newly activated MTOCs at the cell equator (Hagan and Hyams, 1988; Horio et al., 1991). Mitotic chromosome behavior is also representative of that in higher systems as centromere DNA sequences congress to form a metaphase plate before anaphases A and B (Funabiki et al., 1993).

After characterizing the α- and β-tubulin genes (for review see Yanagida, 1987), we isolated the fission yeast γ tubulin gene, *gtb1*$^+$ by virtue of its identity to the *Aspergillus nidulans* γ tubulin gene (Oakley and Oakley, 1989) and showed that it is essential for spindle function (Horio et al., 1991). We have also reported the identification of two fission yeast loci which affect mitotic microtubule patterns in an ostensibly similar fashion when mutated (Hirano et al., 1986; Hagan and Yanagida, 1990). One of these genes, *cut7*$^+$, encodes a potential mitotic microtubule motor protein that is a component of the nuclear division apparatus required for mitotic microtubule interdigitation (Hagan and Yanagida, 1990, 1992; Hagan, I., K. Tanaka, and M. Yanagida, unpublished observations). Here we describe the characterization of the second spindle formation gene *sadl*$^+$ (spindle architecture disrupted [previously referred to as *ts549* (Hagan and Yanagida, 1990]).

The data indicated that the *sadl*$^+$ gene encodes an essential protein with predicted molecular mass of 58 kD which associated with the SPB. When fission yeast protein extracts were run on SDS-PAGE, the protein migrated as two distinct bands at 82 and 84 kD. The predicted amino acid sequence of Sadl contained three features of note: an amino terminal acidic region, a 19–amino acid hydrophobic stretch, and a potential cdc2 phosphorylation site consensus sequence. If expressed at elevated levels, Sadl protein accumulated at the nuclear periphery as well as the SPB. Deleting the gene or gross overproduction resulted in the same microtubule distribution as the reduction of Sadl protein levels in the *sadl.1* mutant, i.e., a mixture of phenotypes as most cells were unable to form a spindle but others assembled nonfunctional ones. We discuss the possibilities that Sadl may help to anchor the SPB in the nuclear membrane or act as a docking point for motor proteins.

Materials and Methods

Strains and Cell Culture

The following strains were used: *h*^{90}, *972h*$^-$, *HM123 (leul.32 h*$^-$) (Gutz et al., 1974) *nuc2.663 leul.32 h*$^-$ (Hirano et al., 1988), *sadl.1 leu.32 h*$^-$ (formerly *ts549*) *sadl.1 leul.32 his2 h*$^+$ (Hagan and Yanagida, 1990), and *leul.32/leul.32 ade6.M210/ade6.M216 his2*$^-$*/his2*$^-$ *ura4.dl8/ura4.dl8 h*$^+$*/h*$^-$ diploid. Cells were cultured in either rich YPD or minimal EMM2 media (Gutz et al., 1974; Moreno et al., 1990) at the temperatures indicated in the text. For mating and meiotic induction, cells were grown in SSL media at 25°C plus nitrogen, washed in SSL, and incubated in SSL media (Egel, 1971) at 25°C for 9–13 h. Synchronous cultures were generated with a JE-5.0 elutriator rotor (Beckman Instrs., Fullerton, CA).

Genetic Manipulations

Standard fission yeast genetic (Gutz et al., 1974; Moreno et al., 1990) and molecular (Sambrook et al., 1989) techniques were used throughout. The plasmid psadl.1 was isolated by complementation of the *sadl.1* temperature-sensitive defect after transformation with a genomic library in a LEU2 based fission yeast vector (Samejima and Yanagida, 1994). Subcloning the insert defined a minimal 2.1-kb BamHI/PstI insert necessary for complementation in plasmid psadl.10 (Fig. 2 *a*). The BamHI–PstI fragment was inserted into Bluescript to make plasmid pssdl and the DNA sequence of the entire fragment was determined independently in either direction. This indicated that the reading frame extended beyond the carboxy-terminal PstI site. The 250 nucleotides distal to this site were therefore sequenced to determine the 3′ sequence of the gene. To generate the fragment for gene deletion two copies of the *ura4*$^+$ gene were inserted between the 5′ HindIII site (at position 468 in Fig. 2 *b*) in pssdl and that 3′ to the gene in the Bluescript polylinker. Subsequently the XhoI–XhoI fragment from plasmid psadl.7 was inserted into the XhoI site of the polylinker in an orientation relative to the *sadl*$^+$ BamHI–HindIII fragment that corresponded to that in genomic *sadl*$^+$ to make plasmid pdsadl.2. The BamHI–PstI fragment pdsadl.2 was identical to the similar region of the genome with the exception that the region from nucleotide 469 to 2259 in Fig. 2 *c* was replaced by two copies of the *ura4*$^+$ gene. This was used to replace one genomic copy of *sadl*$^+$ in a diploid strain by homologous recombination (as determined by Southern blotting using the region from the *sadl*$^+$ distal PstI site to the second BamHI site as a probe).

To place the *sadl*$^+$ gene under the control of the inducible *nmt1*$^+$ promoter (Maundrell, 1993), the BamHI–SalI fragment of pssdl was inserted into BlueScript and the presumptive ATG indicated in Fig. 2 *c* was mutated in vitro by site directed mutagenesis to an NdeI site in plasmid pssd6 to generate plasmid pssd6*. The entire insert was sequenced to verify that no additional changes had taken place. The polylinker XhoI site of pssd6* was converted to a BamHI site by blunt end ligation of a BamHI linker into the cut plasmid. Subsequently, the SalI fragment of psadl.7 including the vector 2 μ and LEU2 sequences were inserted into pssd6* to generate full-length *sadl*$^+$ gene in plasmid pSI1. pSI1 can suppress the *sadl.1* mutation. The pSI1 large NdeI–BamHI fragment was inserted into the NdeI–BamHI site of pREP1 to generate pSI2. psI2 was cleaved with XhoI, blunted, ligated with BamHI linkers, cleaved with BamHI, and religated to generate plasmid pSI3 in which the *sadl*$^+$ gene that is under the control of the *nmt* promoter contains only 100 nucleotides of downstream sequences before the *nmt* polyadenylation signal. pSI3 can suppress the temperature sensitivity of *sadl.1* mutants when uninduced (basal expression from the wild-type *nmt* promoter is often sufficiently high to suppress mutant function).

Generation of Anti-sadl Antibodies

To generate full-length Sadl protein in bacteria to use as an immunogen, the NdeI–BamHI fragment from pSI3 was inserted into the NdeI–BamHI sites of pET-3c (Studier et al., 1990). Despite taking all precautions described in Studier et al. (1990) full-length protein was not detected. Therefore fusion proteins containing the regions NH_2 and COOH-terminal to the BglII site were constructed, SadlFP2 and SadlFP3, respectively. To construct SadlFP2, the 466–nucleotide NdeI–BglII fragment from pSI3 was inserted into NdeI BamHI-digested pET-3c. SadlFP3 was made by inserting the 1.5-kb BglII–BamHI fragment from pSI3 into the BamHI site of pET-3a so that the *sadl*$^+$ open reading frame was inserted in frame with the T7 gene 10 encoding sequences in the vector. SadlFP3, migrated with the expected molecular mass of 43 kD, while the NH_2-terminal one, SadlFP2, migrated some 10–15 kD more slowly than expected from the amino acid sequence prediction alone.

SadlFP3 was incorporated into inclusion bodies upon induction. To purify SadlFP3 for use as an immunogen, or for affinity purification of antibodies from sera, inclusion bodies were purified from induced *E. Coli* strain *BL21* bearing pSadlFP3 and plysS$^+$ (Studier et al., 1990) and subjected to preparative SDS-PAGE. SadlFP3 was subsequently electroeluted from the relevant gel slice in phosphate buffer (100 mM $NaPO_4$ 0.1% SDS, pH 7.2)

and the SDS removed by passage through an Ampure DT column (Amersham Corp., Arlington Heights, IL).

Sad1FP3 was used to generate two rabbit polyclonal sera (Harlow and Lane, 1988) which were affinity purified with nitrocellulose immobilized Sad1FP3 and concentrated to make antibody preparations cAP9 and cAP10. Protein blotting (Harlow and Lane, 1988) using ECL detection systems (Amersham Corp.) and immunofluorescence microscopy with antibodies purified from various bleeds from each animal showed that all antibody preparations recognized the SPB and the doublet at 82 and 84 kD described in the text. However, only antibodies from the second bleed from rabbit 9 (AP9.2 [affinity-purified antibodies from Rabbit 9 bleed 2]) did not give background bands on protein blots and were therefore used for all applications presented in this paper. Antibodies were concentrated from the elution buffer by centrifugation in Sartorious Centristart tubes (cut off 20,000) before use in immunofluorescence (concentrated AP9.2–cAP9.2).

Preparation of Fission Yeast Protein Extracts

Fission yeast protein extracts were prepared as described in Moreno et al. (1990).

Immunolocalization

TAT1 anti-α-tubulin antibody (Woods et al., 1989) or affinity-purified Sad1 antibodies (cAP9.2) were used to visualize microtubules and Sad1 protein, respectively, by immunofluorescence microscopy which used combined aldehyde fixation (Hagan and Hyams, 1988). Double staining was achieved by incubation in mixtures of both primary and secondary antibodies. Similar staining patterns were observed when 4% formaldehyde or plunging into −70°C. Methanol was used as alternative fixation approaches (data not shown). Color images were produced by image capture using a Hamamatsu SIT Camera and C2400 processor for capturing the information from a single fluorochrome into a modified NIH image software package (Improvision: Coventry UK) on a MacIntosh Quadra 950 2/230 and merged in Adobe photoshop.

Results

Spindle Formation and Function Is Defective in the sad1.1 Mutant

Our previous analyses suggested that the temperature-sensitive *sad1.1* mutation (previously referred to as *ts549*) affects the formation of the mitotic spindle (Hagan and Yanagida, 1990). Three defective phenotypes were seen when an asynchrous *sad1.1* culture was shifted to the restrictive temperature of 36°C: (*1*) a "V" or "X" shaped tubulin-

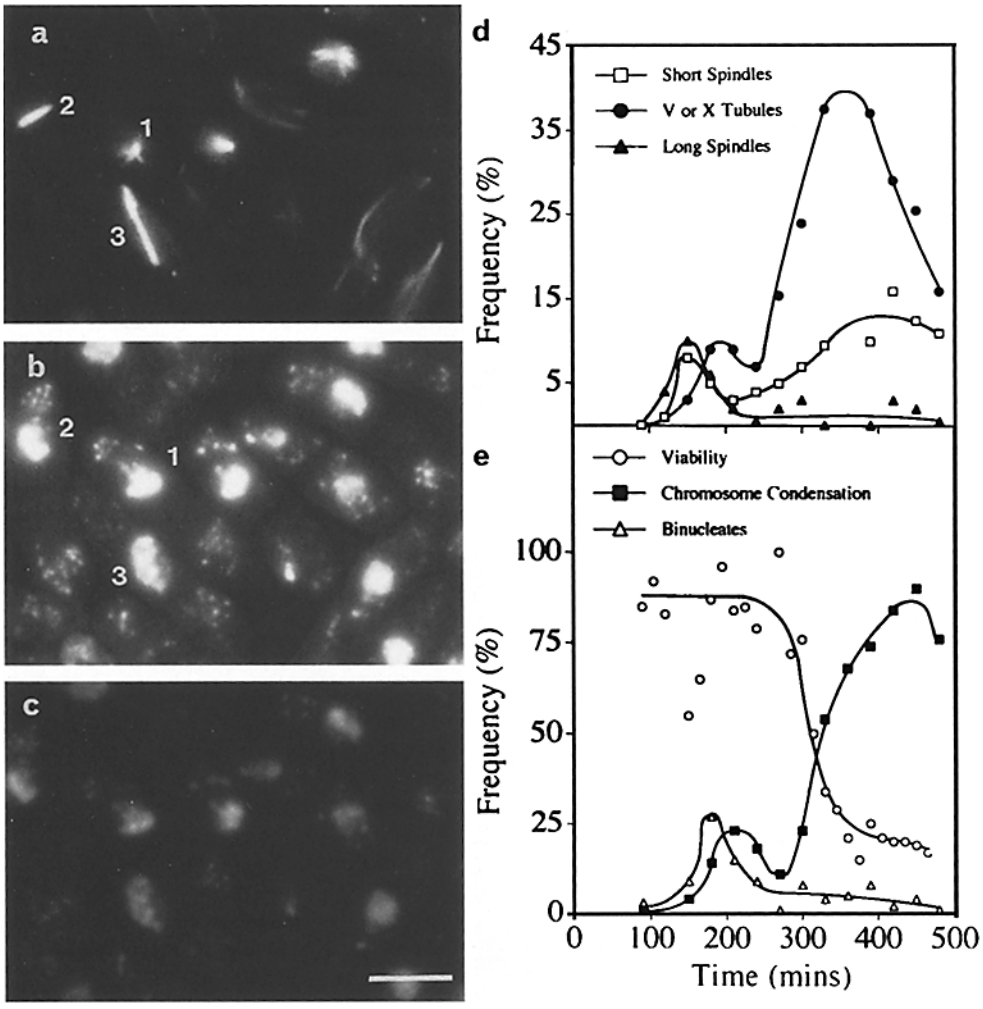

Figure 1. The predominant defect in *sad1.1* mutant cells is the inability to form the mitotic spindle. (*a–c*) Asynchronous *sad1.1* mutant cells after incubation at the restrictive temperature for 6 h. Cells were grown to early-log phase at 25°C in rich medium and shifted to 36°C for 6 h and prepared for anti-tubulin immunofluorescence. *a* shows the anti-tubulin immunofluorescence image, *b*, a combined DAPI and phase contrast image, and *c*, DAPI on its own. The three classes of defect seen are indicated by number: (*1*) accompanying condensed chromosomes and a lack of spindle formation resulting in microtubules extending from a single point (*Xs*); (*2*) short spindles with condensed chromosomes; (*3*) elongating spindles that fail to segregate their condensed chromosomes. (*d* and *e*) Phenotypic analysis of a synchronous *sad1.1* mutant culture. *sad1.1* cells were grown at 25°C and synchronized in G2 of the cell cycle by centrifugal elutriation and incubated at 36°C for the remainder of the experiment (control cultures incubated at 25°C gave a septation peak of 65% after 2.5 h as determined by calcofluor staining). The relative frequencies of each of the three phenotypic classes of microtubule staining seen in panels *a–c* are shown in *d* (-□-) short spindles, (-▲-) spindles longer than the diameter of an interphase nucleus, (-●-) aberrant "V" or "X" staining microtubule-staining structures. *e* shows cell viability (-○-), the chromosome condensation index (-■-), and the frequency of binucleate cells (-△-) in the same culture. These data are derived from a single experiment, however duplicate experiments yielded essentially identical data. Bar, 5 μm.

staining pattern at the base of which chromosomes often cluster (from here on these structures will be referred to as "Xs"); (*2*) brightly staining short spindles with condensed chromosomes; (*3*) elongate spindles on which the chromosomes have failed to segregate (Fig. 1, *a–c*; cells *1–3*, respectively).

To clarify this mixed phenotype, we pursued a detailed characterization of the ts^- defect in a *sadl.1* culture synchronized with respect to cell cycle progression. Synchronization was achieved by centrifugal elutriation and when the cells were in early G2 phase of the cell cycle, the culture temperature was shifted to the restrictive temperature of 36°C. Aliquots were periodically removed and used to determine cell viability or processed for anti-tubulin immunofluorescence microscopy. The data represented in Fig. 1, *d* and *e* indicated that a small but significantly proportion of mitoses in the first cycle after shift (which peaks at 150 min) are defective, as indicated by the transient chromosome condensation and low levels of X's. Cell viability is only marginally affected in the first division. As cells entered the second round of nuclear division (which peaks at 370 min), there was a significant increase in the proportion of the population showing defective mitoses and viability rapidly decreased (greater than 80% lethality). While the majority of these abnormal cells contained Xs, a small, but significant, proportion contained ostensibly normal spindles. Most were short but some were clearly elongating, however in such cases the chromosomes failed to segregate. Thus, when shifted in G2 phase of the cell cycle *sadl.1* cells were able to complete one nuclear division with reduced efficiency, before exhibiting mixed lethal mitotic defects with a predomination of spindle formation defects in the second division after the temperature shift. The predominant defect was an inability to form the mitotic spindle.

sadl$^+$ *Gene Characterization*

By the construction of a diploid strain that was heterozygous at the *sadl.1* locus, we were able to determine that *sadl.1* is a recessive mutation. We therefore cloned the *sadl*$^+$ gene

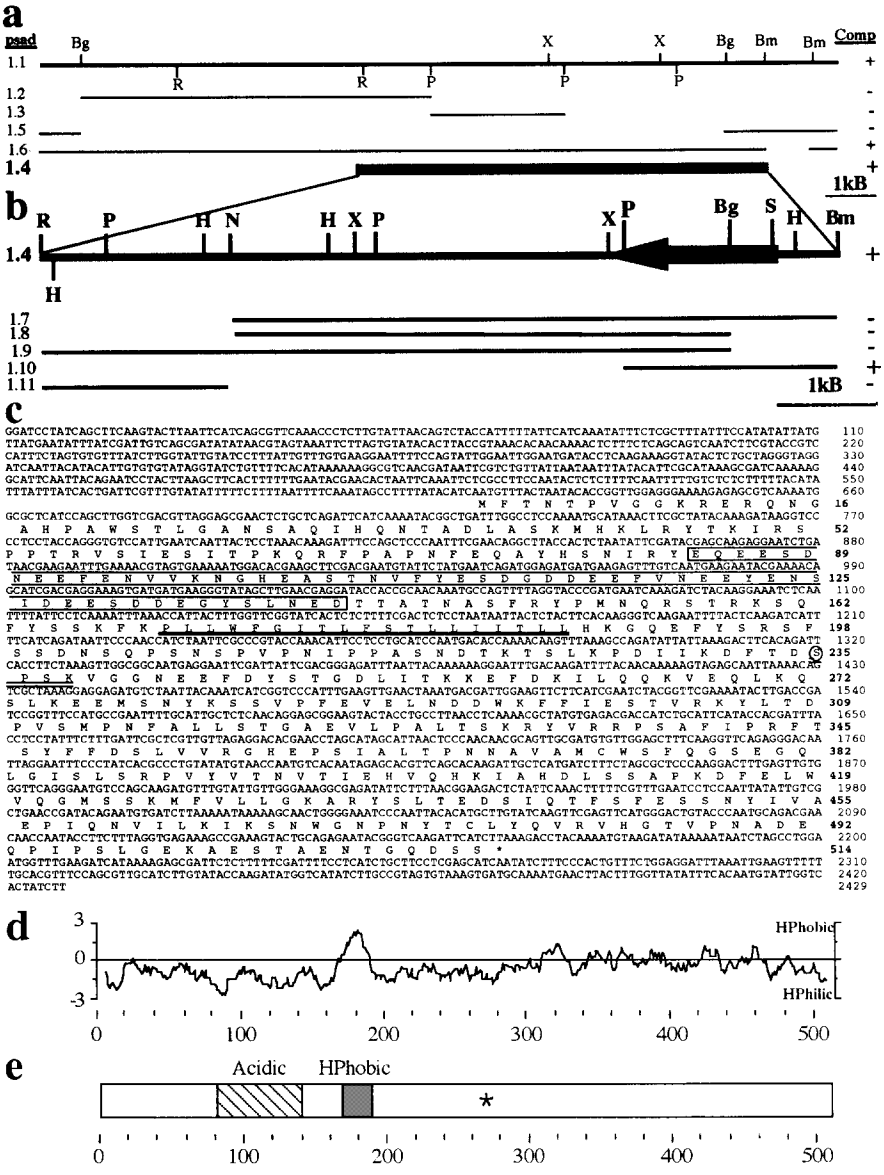

Figure 2. Molecular identification and characterization of the *sadl*$^+$ gene. (*a* and *b*) Plasmid psadl.1 was isolated by transformation of a *sadl.1* mutant culture with an *S. pombe* gene bank (Samejima and Yanagida, 1994) and the resulting plasmid was subcloned to identify the minimum fragment required for complementation as that in psadl.10. Plasmid name is represented on the left of the figure, while its ability to complement is shown on the right hand side. The scale for each panel is indicated, that for panel *b* is twice that in panel *a*. Restriction enzyme cleavage sites are as follows: *Bg*, BglII; *Bm*, BamHl; *H*, HindIII; *N*, NdeI; *P*, PstI; *R*, EcoRV; *S*, SalI; *X*, XhoI. (*c*) The DNA sequence of psadl.10 (*b*) and 200 base pairs from the PstI site was determined and translated. Boxed amino acids indicate a highly acidic region between residues 83 and 141: single underscoring highlights the hydrophobic region identified in *d*: double underscoring indicates a potential cdc2 phosphorylation site with the potentially phosphorylated serine circled. (*d*) A Kyte Doolittle plot of hydrophobicity with an access window of 15 residues. Note the hydrophobic region between 169 and 178. (*e*) A summary of the information gained from the primary amino acid sequence of *sadl*$^+$, acidic, and hydrophobic regions are indicated while a $p34^{cdc2}$/cyclin B phosphorylation consensus site is indicated by an asterisk. These sequence data are available from EMBL/GenBank/DDBJ under accession number x85105.

by complementation of the ts^- mutant defect with a fission yeast gene bank. Two out of 100,000 transformants were capable of growth at the restrictive temperature and contained identical plasmids. These sequences directed integration to within less than 1 cM of the *sadl.1* mutation (PD:47 NPD:0 TT:0) and thus contained the *sadl*$^+$ gene. Subcloning localized the supressing sequences to a 2.1-kb Bam PstI fragment in plasmid psadl.10 as indicated in Fig. 2, *a* and *b*. Sequence determination of this and neighboring DNA indicated the presence of one continuous open reading frame that extended 27 nucleotides beyond the PstI site. The complete nucleotide and predicted amino acid sequences of the sequenced region are shown in Fig. 2 *c*.

The *sadl*$^+$ gene sequence predicted a 514–residue 58-kD protein that has a number of notable motifs as depicted in Fig. 2, *c–e*. 43% of the residues between position 83 and 141 are acidic (boxed region in *c*): Hydrophobicity plots (Fig. 2 *d*) indicated a short stretch of 19 hydrophobic residues from position 170 to 189 and there is a potential $p34^{cdc2}$/cyclin B phosphorylation consensus site at position 236 (*asterisk* in Fig. 2 *e*).

Deletion and Overexpression of the sadl$^+$ *Gene Confers a Phenotype Similar to that of the sadl.1 Mutant*

To determine the phenotypic consequences of a complete lack of the *sadl*$^+$ gene product, we replaced the sequences starting from the HindIII site, 141 nucleotides upstream of

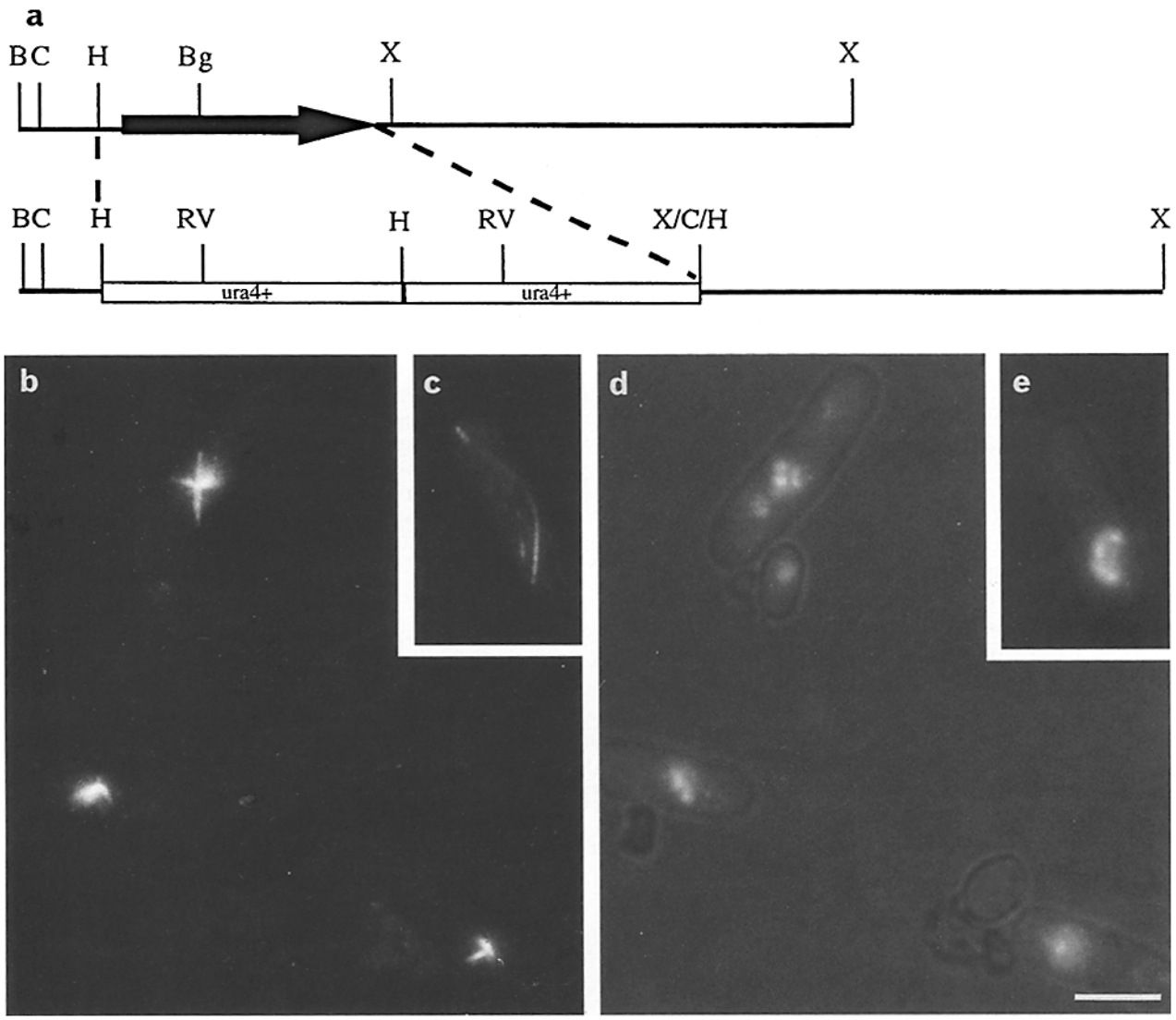

Figure 3. Deletion of *sadl*$^+$ confers a phenotype similar to that of the *sadl.1* mutant. (*a*) A schematic representation of the replacement of the genomic copy of the chromosomal *sadl*$^+$ gene with two copies of the auxotrophic *ura4*$^+$ gene in the cells shown in *b–e*. Capital letters signify restriction sites *B*, BamHI; *Bg*, BglII; *C*, ClaI; *H*, HindIII; *RV*, EcoRV; *X*, XhoI. The arrow indicates the coding region and its direction of transcription. (*b–e*) Spores harvested from a culture of diploid cells in which one copy of the *sadl*$^+$ gene had been replaced with two copies of the *ura4*$^+$ gene were inoculated into medium lacking uracil and incubated at 33°C. The germinating spores went through one successful mitotic division around 13 h before arresting in the second division at the 16-h time point at which time they exhibited the phenotypes shown in the *b–e* ([*b* and *c*] anti-tubulin immunofluorescence: [*d* and *e*] DAPI/phase contrast). Cells arrested with either early spindle formation defects (*b* and *d*) or elongating spindles on which the chromatin failed to segregate (*c* and *e*). Bar, 5 μm.

the *sadl*$^+$ gene, to the XhoI site, 100 nucleotides downstream of the termination codon with two copies of the *ura4*$^+$ gene on one chromosome in a diploid strain lacking any *ura4*$^+$ sequences. This generated the allele *sadl.dl* (Fig. 3 *a*) (Grimm et al., 1988). Gene replacement was confirmed by Southern blotting (data not shown). The resultant diploid cells were sporulated and the spores germinated in minimal medium in the absence of uracil. Spores containing a wild-type copy of the gene do not contain the *ura4*$^+$ gene so they were unable to grow, whereas as those in which it had replaced the *sadl*$^+$ gene did not require uracil for growth and germinate normally.

sadl.dl spores were able to undergo one cell division before arresting with a phenotype similar to *sadl.1* mutant cells. Most cells were unable to form a normal mitotic spindle (Fig. 3, *b* and *d*) while others formed spindles on which chromosomes failed to separate (Fig. 3, *c* and *e*). Some chromosomes fail to associate with the spindle.

To determine the consequences of gross *sadl*$^+$ overexpression the gene was placed under the control of the inducible promoter of the *nmtl*$^+$ gene (Maundrell, 1990) in plasmid pSI3. Removal of thiamine turned on *sadl*$^+$ transcription to give Sad1 protein levels roughly two orders of magnitude greater than normal and resulted in a lethal phenotype similar to that seen in the *sadl.1* and *sadl.dl* mutants with some cells being able to form defective spindles but most being unable to form a spindle at all (data not shown).

Sad1 Specific Antibodies

Antibodies were raised to a bacterial fusion protein containing the first 12 residues of the T7 gene 10 product fused with the carboxy-terminal 360 residues of the *sadl*$^+$ gene product. Two different antisera were raised to this polypeptide. Affinity purification with the same fusion protein, Sad1FP3, yielded antibodies from each sera which recognized two bands after separation by SDS-PAGE, migrating at 82 and 84 kD (Fig. 4, lane *1*).

That these bands represented the *sadl*$^+$ gene product (Sad1) was demonstrated by a number of criteria: increasing *sadl*$^+$ levels by the introduction of multicopy plasmids, psad1.1 and psad1.10 (Fig. 2, *a* and *b*), containing the *sadl*$^+$ gene resulted in 10- and 20-fold increases in the levels of each band (Fig. 4, lanes *2* and *3*); induction of transcription from the inducible *sadl*$^+$ gene on plasmid pSI3 resulted in a 100–200-fold increase in the levels of both the 82- and 84-kD bands (unpublished observations), in the early stages of such induction, when protein levels are elevated twofold, no difference in molecular mass could be detected between the induced and uninduced bands (Fig. 4, lanes *4* and *5*).

Anti-Sad1 Antibodies Recognize the SPB Throughout the Mitotic Cell Division Cycle

Antibodies affinity purified from either antisera gave identical patterns when used to determine the cellular location of Sad1 by immunofluorescence microscopy. Dependent upon cell cycle stage, one or two dots were seen on the nuclear periphery (Fig. 5, *a–c*). Generally in interphase, when microtubules are entirely cytoplasmic, a single dot was always associated with a cytoplasmic microtubule (Fig. 5, *a–c*), while mitotic cells always contained two dots, one at either end of the spindle, the location of the mitotic microtubule-organizing

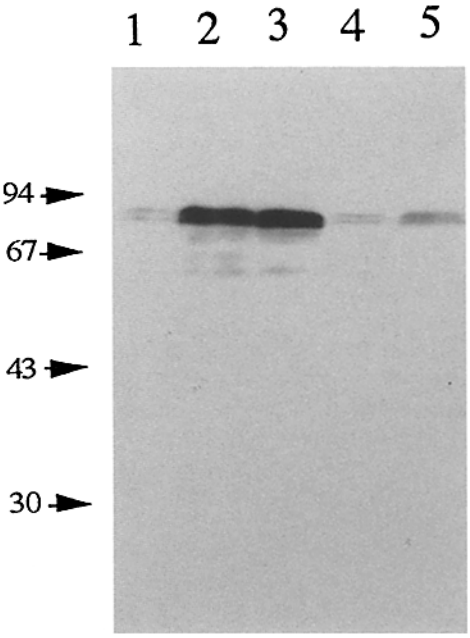

Figure 4. Antibodies raised to, and affinity purified with, bacterially produced Sad1 fusion proteins recognize two bands at 82 and 84 kD. Antibodies (cAP9.2) affinity purified from sera raised to bacterially produced Sad1 fusion proteins recognized two bands at 82 and 84 kD on protein blots of SDS-PAGE of fission yeast protein samples (lane *1*). The intensity of both bands was increased 10-fold and 20-fold in strains containing the psad1.1 and psad1.10 plasmids, respectively (lanes *2* and *3*). Additionally, the intensity of both bands increased in a strain harboring pSI3 (containing the *sadl*$^+$ gene under the control of the inducible *nmt* promoter) upon induction by removal of thiamine from the medium (lane *4* uninduced, lane *5* induced). The sample for lane *5* was taken after 11 h incubation at 33°C without thiamine, when the level of induction was very low. Sampling at later time points indicated that Sad1 levels rise to be two orders of magnitude greater than that seen in wild-type after 18 h (data not shown). Protein levels are identical in all lanes.

center, the SPB. To clearly demonstrate the juxtaposition of Sad1 staining and the spindle termini, we have superimposed false color images of DAPI, anti-Sad1, and anti-tubulin images in Fig. 6. One novel observation with the antibodies was that at the early stages of mitosis one can easily detect separation of the SPBs, and thus spindle formation before the complete loss of interphase cytoplasmic microtubules (Fig. 5, *d–f*).

While the location of the dots to the end of the spindle (Fig. 6) and the spindle formation defects upon manipulation of the *sadl*$^+$ gene suggested that the antibodies were recognizing the SPB, we have been unable to detect any association with the central microtubule-organizing centers activated at the end of the mitosis (Hagan and Hyams, 1988) (Fig. 5, *g–l*), therefore, unlike γ-tubulin, Sad1 is not a ubiquitous component of fission yeast MOTCs (Horio et al., 1991).

Microtubules were depolymerized to determine whether Sad1 localization to the SPB is microtubule dependent. Whether we incubated cells on ice for 25 min (Fig. 7, *a–c*), or exploited the β-tubulin mutation *nda3.KM311* (Funabiki et al., 1993) to depolymerize microtubules, Sad1 staining was unaffected.

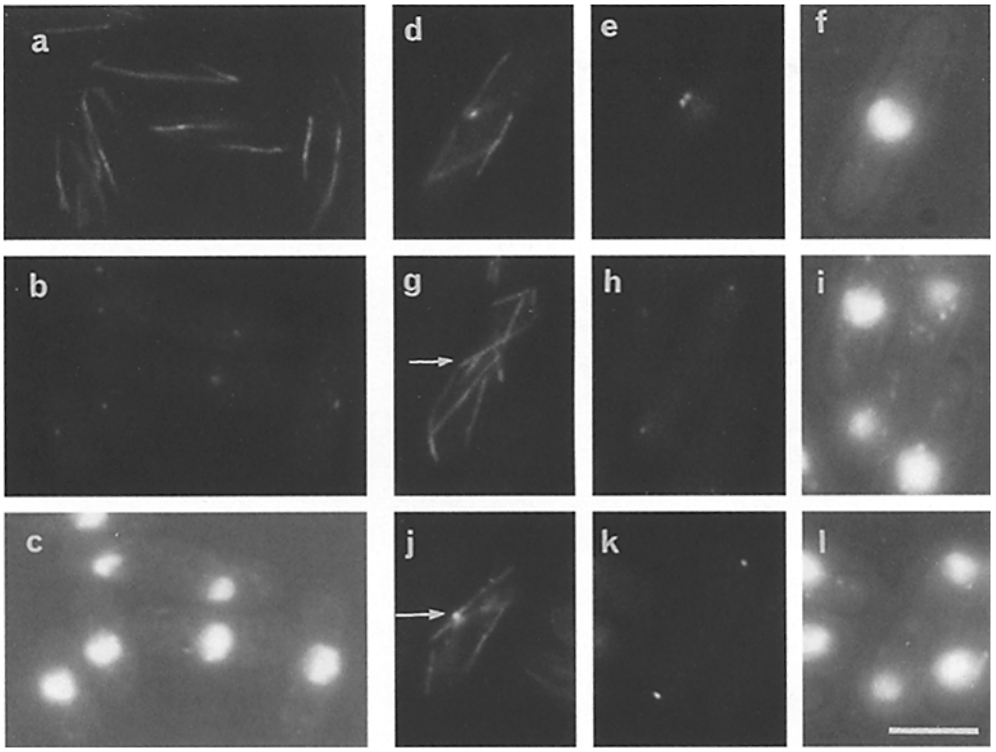

Figure 5. Anti-Sadl antibodies recognize the SPB but not the MTOC responsible for the nucleation of microtubules immediately after the completion of anaphase B. Wild-type cells were grown to mid-log phase in rich YPD media at 33°C before processing for immunofluorescence. Three images of each cell are presented sequentially. Images (*a*, *d*, *g*, and *j*) show microtubules, (*b*, *e*, *h*, and *k*) Sadl staining, and (*c*, *f*, *i*, and *l*) combined DAPI and phase contrast. *a–c* show one mitotic and several interphase cells. Sadl staining was found in a position that correlated with the end of the spindle in *a* and was always associated with both the nucleus and a cytoplasmic microtubule in interphase cells. The strong tubulin signal between the two sadl dots in *d–f* suggested the presence of a very early spindle. The cells in *g–l* demonstrated that while sadl antibodies stain the SPB throughout the mitotic cell cycle, they do not recognize the central MTOCs activated at the end of anaphase at the cell equator (indicated by *arrows*). Bar, 5 μm.

Given that the anomalous behavior of chromosomes in spindles after *sadl*$^+$ manipulation may indicate a kinetochore function for Sadl and that a prolonged metaphase might lead to Sadl kinetochore accumulation to detectable levels, we localized Sadl after metaphase arrest using the *nuc2.663* temperature-sensitive mutation (Hirano et al., 1988, 1990). We could detect no kinetochore staining even after depolymerization of the metaphase microtubules (Fig. 8), indicating that there is no Sadl kinetochore accumulation or masking of kinetochore bound Sadl by microtubule kinetochore association (Fig. 8). Notably after microtubule depolymerization, the SPBs were closely apposed indicating the presence of some restraining force that may arise from the elasticity of the nuclear membrane or the action of microtubule motor proteins (Saunders and Hoyt, 1992).

Moderate Overexpression of Sadl Protein Results in its Localization to the Nuclear Periphery and Distortion of the Nuclear Profile

To extend our analysis of Sadl function, we moderately increased cellular *sadl*$^+$ levels by introduction of a *sadl*$^+$ bearing multicopy plasmid to look for any alterations of staining pattern or SPB behavior (Fig. 9).

In addition to recognizing the SPB, Sadl antibodies stained the nuclear periphery in a third of cells after introduction of the plasmid psadl.1 (Fig. 9, *b* and *f*). Variability in signal intensity from cell to cell in strains bearing genes on 2 μ based multicopy plasmids has been noted previously (Hagan and Yanagida, 1992) and probably reflects variation of plasmid copy number. In many cases the shape of the interphase nucleus was curiously distorted with the SPB at the tip of the distortion (e.g., cells *1–3*) while in other cells the SPB took on a more elongated rod-like morphology (cell *4*), possibly reflecting alteration of SPB structure. While roughly 6% of wild-type interphase cells showed a small degree of nuclear distortion, 13% of interphase cells harboring psadl.1 had distended nuclei and the distortion was generally much more pronounced than in wild-type cells. Cell *5* indicated that despite incorporation of a considerable amount of Sadl into the nuclear periphery mitosis was apparently unaffected. A final point, indicated by cell *6*, is that, despite

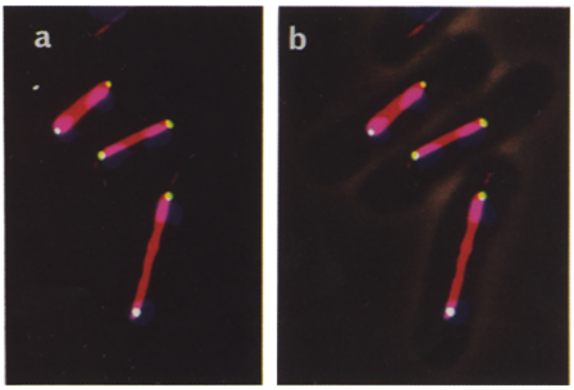

Figure 6. Anti-Sadl antibodies stain the spindle poles. Mid-log phase wild-type cells were stained with DAPI (*blue*) and antibodies against tubulin (*red*) and Sadl (*green*). Images were captured as single fluorescence images and merged to give the image shown in the figure. Note that the only Sadl signal is at the ends of the mitotic spindles which are separating the genomes.

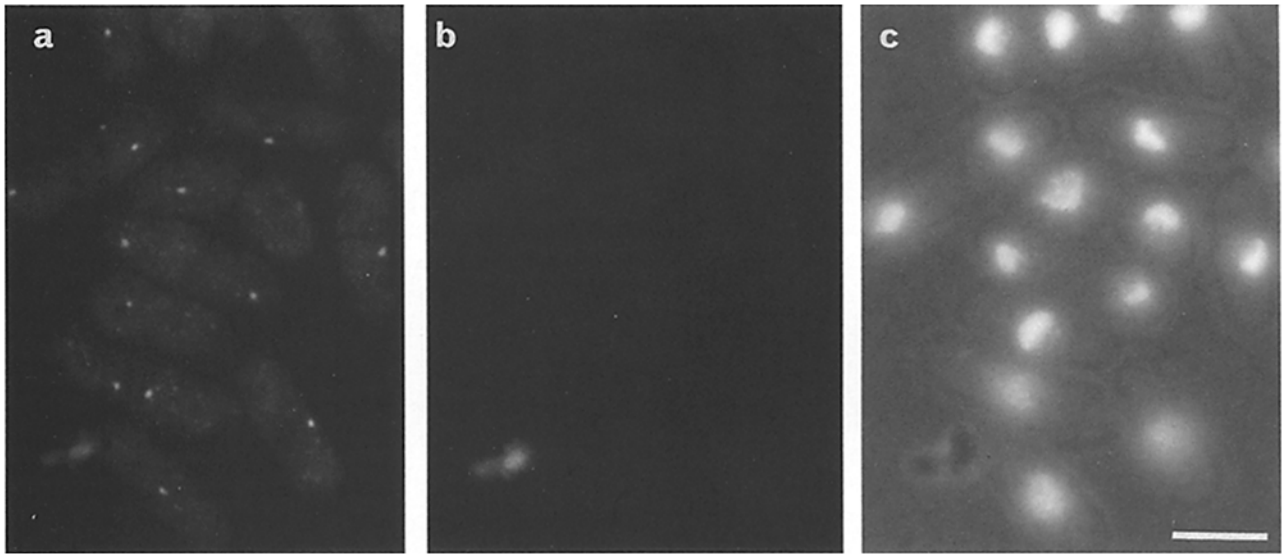

Figure 7. Sad1 localization is independent of microtubule integrity. *a–c* represent images of the same field of wild-type cells. *a* shows Sad1 staining, *b*, TAT1 microtubule staining, and *c*, combined DAPI phase contrast images. Cells were grown to mid-log phase at 33°C in rich YPD media before depolymerization of the microtubules by incubation on ice for 25 min. Cells were fixed by direct addition of ice cold fixative to the culture on ice. Rewarming of cells from ice treatment results in repolymerization of microtubules (data not shown). The data indicated that Sad1 distribution is independent of microtubule integrity. Bar, 5 μm.

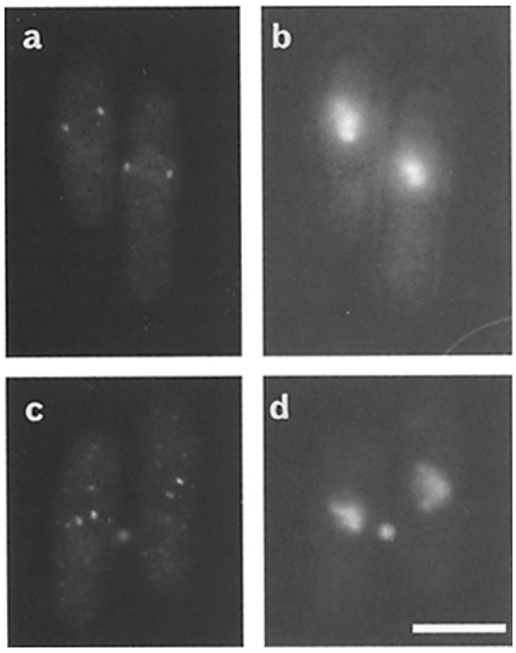

Figure 8. No detectable Sad1 kinetochore staining despite prolonged metaphase arrest and subsequent depolymerization of the microtubules. *nuc2.663* cells were grown in rich YPD media at 25°C to early log phase before the temperature of the culture was shifted to 36°C (the restrictive temperature for *nuc2.663* mutants) and incubated for an additional 3 h in order to affect the *nuc2.663* gene product and lead to mitotic arrest at metaphase. *a* and *c* are anti-Sad1 images while *b* and *d* are the respective DAPI/phase contrast images of the same cells. The cells in panels *c* and *d* have been incubated on ice for 25 min subsequent to *nuc2*^{ts} dependent cell cycle arrest in order to depolymerize the microtubules. In neither case was any additional kinetochore staining visible. Interestingly, the SPBs congress after microtubule depolymerization. Bar, 5 μm.

sufficient overexpression of the protein to drive it into the nuclear periphery, Sad1 failed to associate with the MTOCs at the cell equator which nucleate the post-anaphase array after the completion of anaphase B.

Sad1 Is Thermolabile in the sad1.1 Mutant

To investigate the nature of the *sad1.1* defect, we looked at the Sad1 protein in *sad1.1* mutant cells. Cultures of wild-type and mutant cells were grown to early log phase at 25°C and the temperature of the culture was shifted to 36°C which is the restrictive temperature for cells harboring the *sad1.1* mutation. Samples were taken at 0, 3, and 6 h after the shift and prepared for anti-Sad1 immunoblotting. Both sets of affinity-purified polyclonal antibodies gave identical results. There was no change in either the relative or gross levels of the two Sad1 bands in wild-type cells (data not shown) but by the 3-h time point for the mutant cells, most of the 82-kD band had disappeared and the 84-kD band was noticeably weaker, while at 6 h only an extremely faint 84-kD band is detectable (Fig. 10 *a*).

Immunolocalization of the cells revealed no change in Sad1 distribution in wild-type cells upon temperature shift (data not shown). While the Sad1 signal at 0 h was normal in the *sad1.1* mutant and much fainter at 3 h (Fig. 10, *e–g*), no signal could be detected at 6 h (Fig. 10, *h–j*). In combination with the data in the previous section, such mutant-dependent behavior confirmed that the blotting and immunofluorescence signals are attributable to the Sad1 protein.

Correlation between Alteration of Staining Patterns and Differentiation of SPB Structure and Function

In addition to its mitotic role, the SPB is intimately involved in a number of other events including mitotic nuclear migration in the mitotic cell cycle (Hagan, I., and M. Yanagida,

unpublished observations), meiotic nuclear migration both during karyogamy and a series of presegregation meiotic nuclear migrations, the function of both the reductive and equational meiotic spindles, and the modification of its outer face to initiate spore wall formation from metaphase of the second meiotic division (Robinow, 1977; Hirata and Tanaka, 1982; Chikashige et al., 1994). We therefore stained mating and meiotic wild-type h^{90} cells to determine any changes in Sadl distribution indicative of differentiation of protein function.

Sadl antibodies stained the SPB as a single dot throughout karyogamy (Fig. 11 *a*), presegregation migration, characterized by the typical "horse tail" structure (Fig. 11 *b*), meiosis I (Fig. 11 *c*), and meiosis II (Fig. 11, *d–i*). Staining in meiosis II differed significantly from that at all other stages of the fission yeast life cycle. While the SPB of the prophase spindle stained as a discrete dot (Fig. 11, *d*), as cells progress through prometaphase (Fig. 11 *e*) to metaphase (Fig. 11 *f*), Sadl staining changed from a dot to a cresent. The crescent started to disappear in anaphase A (Fig. 11 *g*) and by mid-anaphase B Sadl staining was a dot once more (Fig. 11 *h*) and remained punctate until spore wall formation was complete (Fig. 11 *i*). These changes in Sadl staining to a crescent shape coincide with well documented changes in SPB structure during meiosis II.

Discussion

Here we describe the isolation of the spindle formation gene *sadl*$^+$ and demonstrate that it encodes an essential protein that associates with the fission yeast spindle pole body.

The sadl.1 Phenotype

We previously identified the *sadl.1* mutation while screening a bank of temperature-sensitive mutants by anti-tubulin immunofluorescence for those which exhibited abnormal spindle structure at the nonpermissive temperature. We showed that mutation of *sadl*$^+$ can lead to a spindle formation defect similar, at the level of immunofluorescence microscopy, to that caused by mutation in the putative mitotic motor protein gene *cut7*$^+$ (Hagan and Yanagida, 1990). Here we extend the phenotypic characterization of the *sadl*$^+$ gene and have shown that while many cells aborted spindle formation with several microtubular bundles extending from a single point, some *sadl.1* mutant cells were capable of forming a short spindle and in some cases this spindle could elongate. Chromosome segregation on these spindles was, however, severely impaired. Phenotypic characterization of the *sadl.1* defect in a synchronous culture indicated that most of these defects were exhibited in the second nuclear division after the temperature shift.

Genetic manipulations demonstrated that *sadl*$^+$ was essential for viability and that *sadl*$^+$ deletion or overexpression led to the same mixed phenotype as seen in *sadl.1* cells. The data suggest that complete loss of Sadl function led to an inability to form a normal spindle while partial impairment of function severely affected spindle function, but not necessarily formation. Similar observations have been made for mammalian and budding yeast MTOC components (Doxsey et al., 1994; Thomas and Botstein 1986; Winey et al., 1991, 1993).

sadl$^+$ Encodes a Protein That Associates with the Spindle Pole Body

Immunofluorescence of cells in the motitic cell cycle demonstrated that Sadl associated with the SPB and not with the central microtubule-organizing centers that are activated at the end of mitosis to reestablish the interphase cytoskeleton. SPB association and a potential role in SPB function was further substantiated by the change in Sadl-staining patterns from a dot to a crescent shape during metaphase of meiosis II as the timing of this change correlates precisely with the well documented differentiation of the outer face of the SPB at this time. Electron microscopic studies have shown that at this stage the SPB becomes much more complex than at any other time in the life cycle as additional layers form and the forespore membrane, which will give rise to the spore wall, extends from the outer most layer (Tanaka and Hirata, 1982; Hirata and Tanaka, 1982; Hirata and Shimoda, 1994).

Mitotic Timing, SPB Function, and Sadl Staining

The ability to observe the spindle pole body throughout the mitotic cell cycle with anti-Sadl antibodies has already considerably advanced our understanding of fission yeast cell biology (Funabiki et al., 1993; Chikashige et al., 1994) and will continue to do so.

Here we have shown that in interphase the SPB is always associated with cytoplasmic microtubules. Given the apparent continuity of the cytoplasmic microtubules which associate with the SPB, the association is presumably not with microtubule termini as in budding yeast but lateral. This raises the possibility that the SPB plays an important role in nuclear positioning. Furthermore, the fact that we observed two Sadl dots either side of strong tubulin staining in the presence of an interphase microtubule cytoskeleton (Fig. 5, *d–f*) suggests that, contrary to previous conclusions (Hagan and Hyams, 1988), early spindle formation occurs before the interphase microtubule cytoskeleton has completely depolymerized. While the most probable basis for this overlap of microtubule classes lies in kinetic differences between the time required for interphase microtubules to depolymerize and the rapidity of spindle formation, it could arise from different signals being required to depolymerize the interphase cytoskeleton and initiate spindle formation once the decision to transit from G2 to mitosis has been taken. Consistent with this possibility, mutations in the cyclin B subunit of the cell cycle regulating kinase complex result in the coexistence of anaphase spindles and cytoplasmic microtubules (Hagan et al., 1988). If this viewpoint is true it casts doubt on the ability to categorize cells as interphase or mitotic based purely upon the presence of cytoplasmic microtubules. The persistence of cytoplasmic microtubules during spindle formation has significant implications for models to account for the initial separation and reorientation of fission yeast SPBs during spindle formation (Hagan and Yanagida, 1992).

Sadl Function

In the absence of electron microscopy, the exact defect in the *sadl.1* strain remains obscure, however considering all the data, it is possible to speculate on a number of potential roles for Sadl.

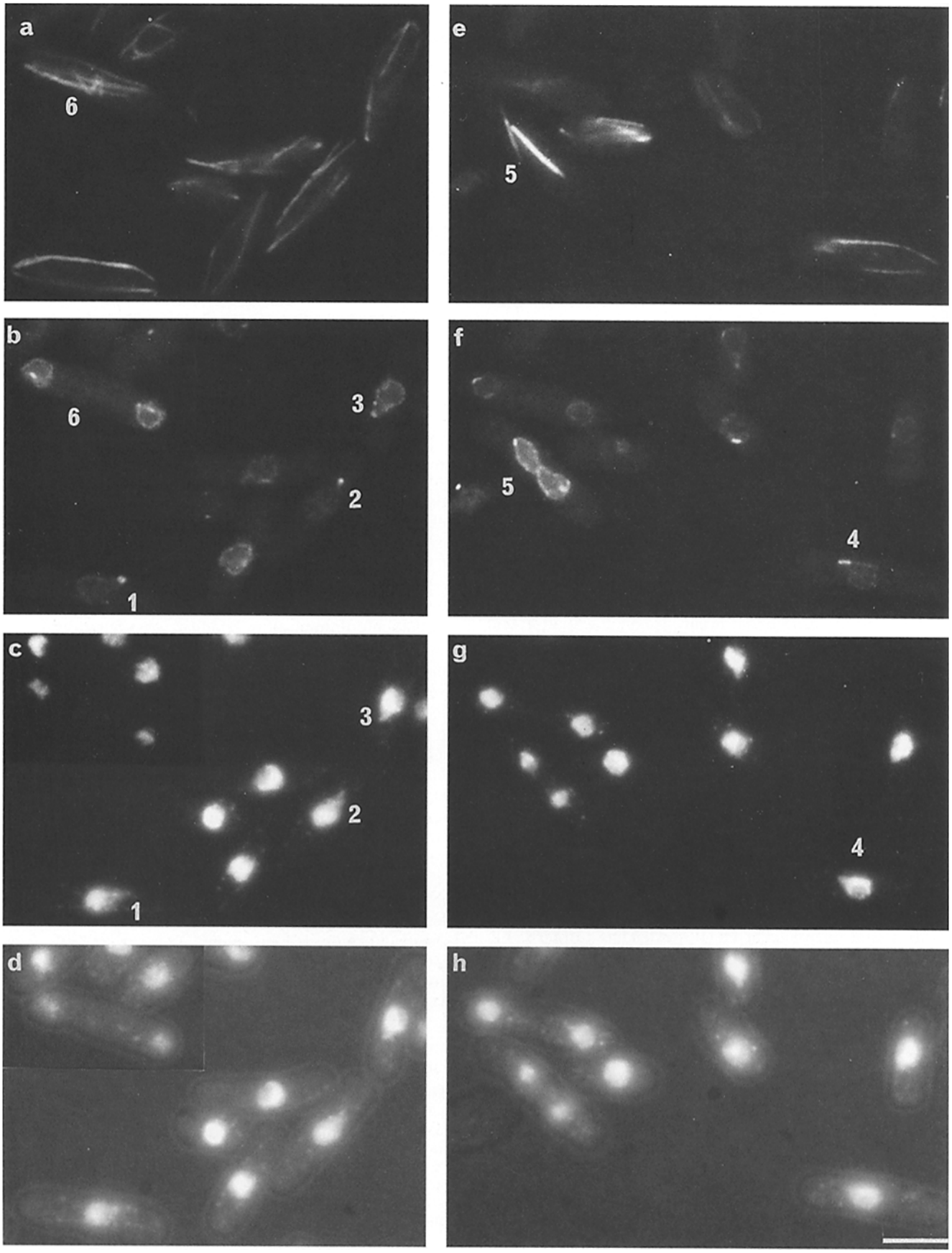
a
6
e
5
b
6
3
2
1
f
5
4
c
3
2
1
g
4
d
h

A Structural Role for Sad1 in the SPB?

While database searches showed that Sad1 is a novel protein, Sad1 localization and primary amino acid sequence data have given considerable insight into Sad1 function. The data have clearly shown that in wild-type cells Sad1 was exclusively associated with the SPB. We have never detected Sad1 in the central MTOCs that are activated at the end of anaphase and reestablish the cytoplasmic interphase array (Hagan and Hyams, 1988; Horio et al., 1991). This differs from γ tubulin which is found in both locations (Horio et al., 1991).

A further hint of Sad1 function was given by the incorporation of excess Sad1 into the nuclear periphery. This suggests either that Sad1 is associating with a nuclear matrix like structure or with the nuclear membrane (which remains intact throughout fission yeast mitosis). The dynamic nature of mitosis and precedents from higher eukaryotes argue against the persistence of a matrix structure throughout mitosis whereas the presence of a hydrophobic 19-amino acid stretch in Sad1 is consistent with nuclear membrane insertion. Studies of budding yeast SPB components have shown that the 20-aa hydrophobic stretch in the SPB protein KAR1 (Rose and Fink, 1987) is sufficient to direct insertion of KAR1/β-galactosidase fusion proteins into the nuclear membrane (Vallen et al., 1992*a*) and that overexpression of the multi-membrane-spanning protein, essential for SPB function, Ndc1p, leads to accumulation in the nuclear periphery (Winey et al., 1993).

If this region of Sad1 is directing membrane insertion an interesting analogy may be drawn. Data suggest that the signals that specify localization to a particular compartment of the Golgi lie within the membrane-spanning domain rather than the luminal sequences, leading Nilsson and Warren to propose that these regions specify localization by directing specific interactions with the transmembrane sequences of other Golgi proteins within the correct compartment and thus determining specific localization (Nilsson et al., 1994). This raises the interesting possibility that the membrane-spanning domains in Sad1 and Kar1p may not be just passive membrane-spanning sequences but may direct interaction with other SPB proteins.

Sad1 as an Anchor for Motor Proteins?

From studies in different mutant backgrounds (Hagan, I., and M. Yanagida, manuscript in preparation) and the facts that in interphase the SPB is always associated with cytoplasmic microtubules, and that overexpression of Sad1 results in the distortion of the nuclear profile with the SPB at the tip of a pointed extension of the nucleus, we may conclude that the SPB is involved in nuclear positioning by migration along cytoplasmic microtubules.

Impairment of this function by excess Sad1 could simply have arisen from altered dynamics of nuclear structure and flexibility due to excess Sad1 association with either the nuclear membrane or the nuclear matrix. Alternatively, the problem may lie in the SPB as Sad1 overproduction may affect SPB structure so that the SPB association, or the function of, the microtubule motors responsible for nuclear positioning during interphase is defective. If the latter, these motors may bind directly to the cytoplasmic face of the SPB via Sad1 as has been suggested for the KAR1 gene of the budding yeast *S. cerevisiae* (Vallen et al., 1992*a*). Production of a KAR1/β-galactosidase fusion protein led to nuclear extensions reminiscent of those seen upon production of excess Sad1 (Vallen et al., 1992*b*). More recently a direct interaction between a budding yeast SPB component CIK1 and a microtubule motor protein, KAR3, has been demonstrated (Page et al., 1994).

Were motors to bind directly to Sad1, we would have to postulate the fulfillment of some additional criteria for motor binding in order to account for the data. If a simple relationship existed one would predict that the entire Sad1 staining nuclear periphery would not be rendered competent to bind with motors and thus microtubules wherever Sad1 is associated. However, this is not seen and the nucleus only associates with microtubules via the SPB when Sad1 is also present in the nuclear periphery. Therefore if Sad1 has any interaction with motors, the motors may be in limited supply, require coassociation with additional SPB components for attachment or prefer to bind to a Sad1 structural configuration found only in the highly organized SPB.

Sad1 at the Kinetochore?

Chromosome disjunction and association with spindles often fail after Sad1 manipulation, possibly suggesting a role of Sad1 at the kinetochore. However, we failed to stain kinetochores with Sad1 antibodies even after manipulations aimed at increasing protein recruitment to the kinetochore.

While Sad1 could be a kinetochore component and the antigen is buried in the chromatin, it is likely that the chromosome migration defects are caused by the influence of Sad1 on spindle structure in general, and reflect a generally weakened spindle through a general affect on MTOC structure (Doxsey et al., 1994).

Figure 9. Sad1 localization in cells containing the *sad1*$^+$ gene on multi-copy number plasmid, psad1.1. The figure shows two fields of cells (*a–d* and *e–h*) from a culture of wild-type cells containing the *sad1*$^+$ gene on a multi-copy number plasmid (psad1.1) grown under selective conditions in minimal medium at 33°C to mid-log phase. For each field is shown, from top to bottom; anti-tubulin microtubule (*a* and *e*), cAP9.2 anti-Sad1 (*b* and *f*), DAPI chromatin (*c* and *g*), and combined DAPI/phase contrast (*d* and *h*) images. In many cells, in addition to the usual SPB staining, staining of the nuclear periphery was apparent. Its intensity varied from cell to cell, probably reflecting variation in the plasmid copy number of 2 μ based plasmids in fission yeast. The nuclei in the cells *1–4* were pointed with a strong Sad1 staining dot at the tip of a DAPI protuberance. The Sad1 staining in cell *4* of *f* was linear rather than punctate. Despite the obviously elevated Sad1 levels cell *5* underwent an apparently normal mitosis, and in cell *6* there was no signal at the position of the central MTOC of the post-anaphase array, verifying the previous conclusion from wild-type images that the protein is not associated with the microtubule-organizing centers responsible for organizing the post-anaphase array. While the only mitotic cell in the figure is cell *5* and it has strong Sad1 staining of the entire nuclear periphery, other cells at a similar mitotic stage had levels varying from wild type to that seen in cell *5*. Bar, 5 μm.

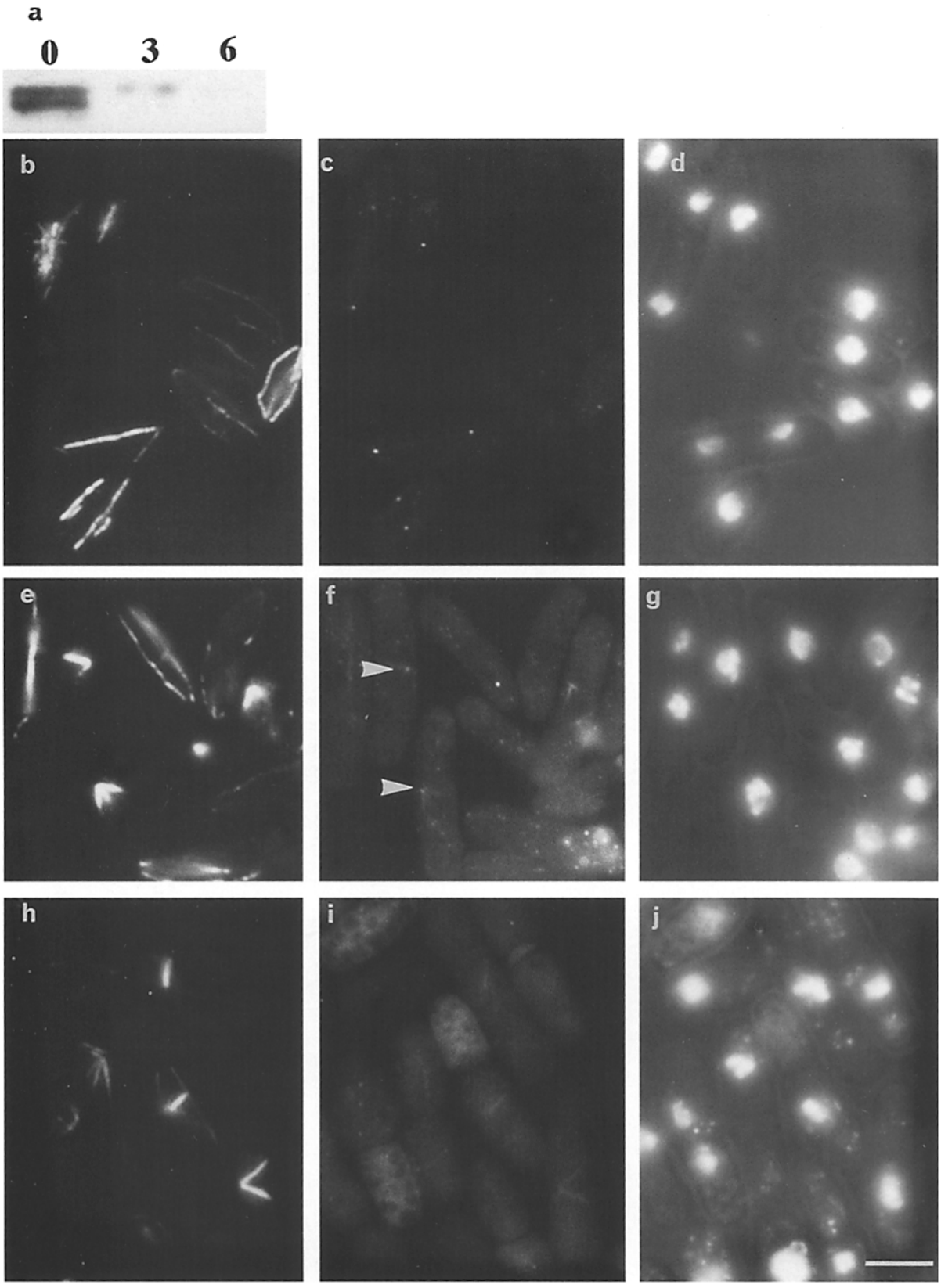

Figure 10. The sad1 signal radically decreases in *sad1.1* mutants at the restrictive temperature. *sad1.1 leu1.32* h^- cells were grown in rich YPD medium to early log phase and the temperature of the culture was shifted from 25°C (permissive for the *sad1.1* mutation) to 36°C (restrictive). Samples were taken for protein blotting at 0, 3, and 6 h after the temperature shift (*a*). The signal radically decreased after 3 h, (that of the lower band being markedly fainter than the upper) and was virtually absent after 6 h, although a faint upper band could be detected upon prolonged exposure of the blot (data not shown). *b*, *e*, and *h* show anti-tubulin, (*c*, *f*, and *i*) anti-Sad1 staining, and (*d*, *g*, and *j*) combined DAPI and phase contrast images of the same fields of *sad1.1* mutant cells. *b–d* are cells before the shift, *e–g* and *h–j*, 3 and 6 h after the shift to the restrictive temperature, respectively. The SPB staining seen at the permissive temperature was indistinguishable from wild-type, while after 3 h, the intensity of the signal was radically reduced and can only be seen upon long exposure when the bleed-through from the tubulin channel is apparent. The arrows in *f* indicate faint Sad1 dots. After 6 h there is no detectable Sad1 signal (although at these exposures, there is significant bleed through from the tubulin channel). Bar, 5 μm.

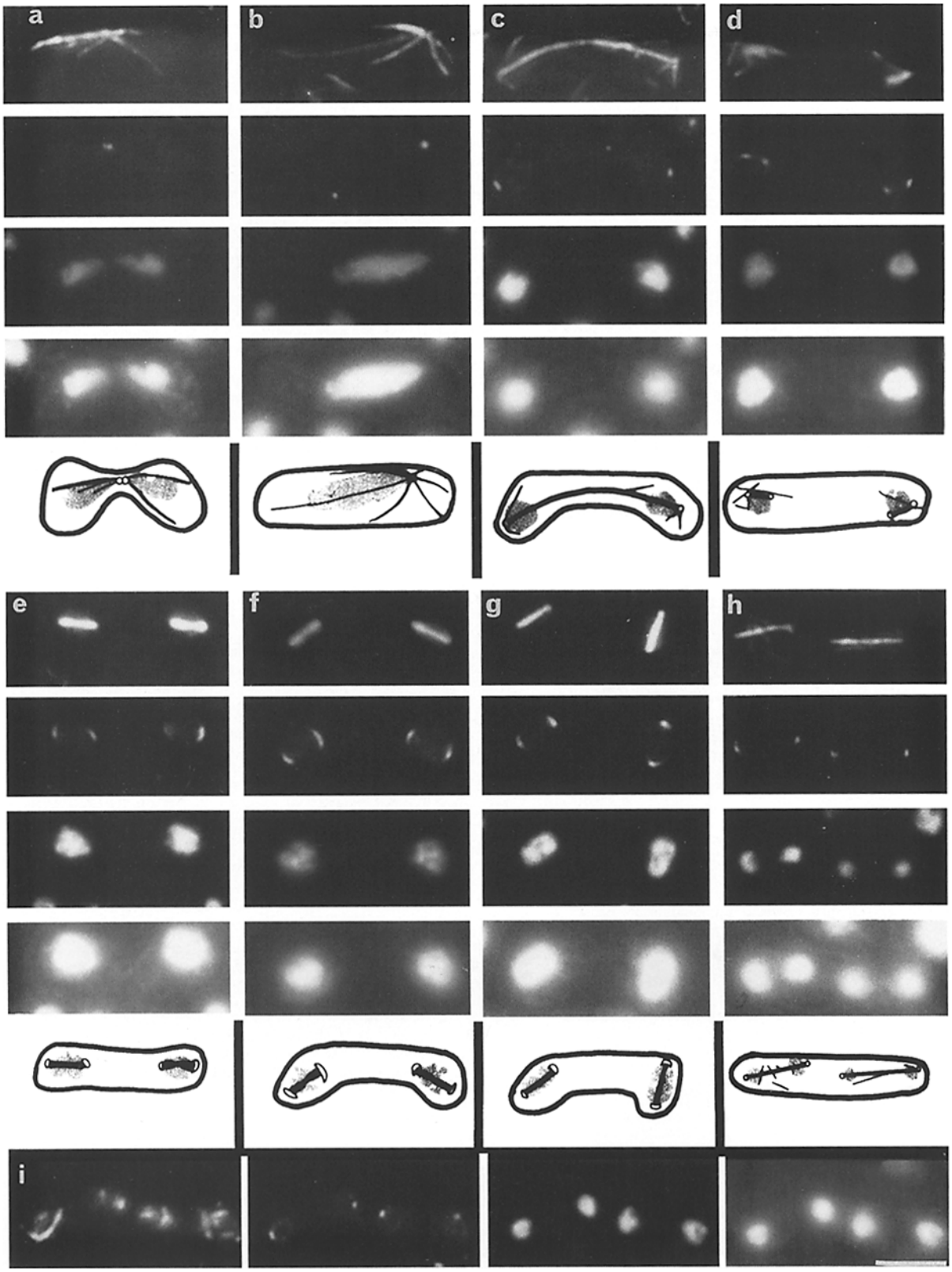

Figure 11. Sad1 antibody staining alters with the differentiation of the SPB during the second meiotic division. The figure shows images of a field of wild-type cells at different stages of meiosis. With the exception of *i*, each cell is represented in five different panels showing, in order: TAT1 staining of microtubules, cAP9.2 anti-Sad1 staining, DAPI staining to reveal chromatin, a combined DAPI/phase contrast image, and a cartoon of the cell to show the relative location of these structures. Panel *i* is similar in arrangement from left to right but has no cartoon representation. (*a*) Karyogamy, nuclei moved along microtubule tracks towards each other. (*b*) After fusion of the two nuclei, the single nucleus underwent considerable movements that are characterized by a "horse tail" structure (Robinow 1977; Chikashige et al., 1994). Subsequently cells entered meiosis I (*c*) and II (*d*). During the progression from prophase to metaphase of meiosis II (*d–f*) Sad1 staining changed from a dot to a crescent. Once anaphase A was initiated the crescent staining diminished (*g*) to return to a dot in mid anaphase B (*h*), a pattern that persisted until encapsulation of the nucleus by the spore wall (*i*). Bar, 5 μm.

Sad1 and the Spindle Pole Body and Cell Cycles

At least two gross alterations of behavior may be anticipated for SPB proteins, one accompanying their incorporation into the new SPB during SPB duplication and the second upon SPB activation during nuclear division. In this context the fact that two Sad1 isoforms are observed by SDS-PAGE is provocative and could reflect SPB cycle or cell cycle modifications. Such modifications could be achieved via phosphorylation by a cell cycle kinase, e.g., $p34^{cdc2}$/cyclin B–dependent phosphorylation of residue 237.

Concluding Remarks

The lack of any visible effects on microtubule dynamics and of any microtubule nucleation from the nuclear periphery upon overproduction along with the lack of Sad1 in the central MTOCs corroborates the conclusions from *sadl* mutation, deletion, or overexpression that it is not directly involved in microtubule nucleation. This favors a structural role for Sad1 rather than a direct role in microtubule nucleation. The potential membrane-spanning domain of Sad1 may indicate a role in SPB integration into the nuclear membrane, perhaps to encircle the SPB with a membrane interfacing molecule thus facilitating SPB integration and migration in the nuclear membrane during SPB separation in spindle formation.

While the *sadl*$^+$ gene itself is of intrinsic interest, antibodies against the Sad1 protein have proved (Funabiki et al., 1993; Chikashige et al., 1994) and will continue to prove, to be a useful tool in fission yeast cell biology as it is the first protein to be localized solely at the fission yeast SPB.

We are grateful to Prof. K. Gull for the generous gift of TAT1 antibody and for use of image processing equipment. We are indebted to Drs. J. Kilmartin, S. Uzawa, I. Samejima, and H. Funabiki and members of the Manchester and Kyoto departments for stimulating discussions.

This work was supported by grants from the Ministry of Education, Science and Culture of Japan (a Specially Promoted Research Position) to M. Yanagida, the International Human Frontier Science Programme Organisation and Cancer Research Campaign to I. Hagan.

Received for publication 28 October 1994 and in revised form 2 February 1995.

References

Ault, J. G., and C. L. Rieder. 1994. Centrosome and kinetochore movement in mitosis. *Curr. Opin. Cell Biol.* 6:41–49.

Belmont, L. D., A. A. Hyman, K. E. Sawin, and T. J. Mitchison. 1990. Real-time visualisation of cell cycle dependent changes in microtubule dynamics in cytoplasmic extracts. *Cell.* 62:579–589.

Buendia, B., G. Draetta, and E. Karsenti. 1992. Regulation of the microtubule nucleating activity of centrosomes in Xenopus egg extracts: role of cyclin A-associated protein kinase. *J. Cell Biol.* 116:1431–1442.

Centonze, V. E., and G. G. Borisy. 1990. Nucleation of microtubules from mitotic centrosomes is modulated by a phosphorylated epitope. *J. Cell Sci.* 95:405–411.

Chikashige, Y., D. Q. Ding, H. Funabiki, T. Maraguci, S. Mashiko, M. Yanagida, and Y. Hiraoka. 1994. Telomere led premeiotic chromosome movement in fission yeast. *Science (Wash. DC).* 264:270–273.

Ding, R., K. L. McDonald, and J. R. McIntosh. 1993. Three-dimensional reconstruction and analysis of mitotic spindles from the yeast *Schizosaccharomyces pombe*. *J. Cell Biol.* 120:141–151.

Doxsey, S. J., P. Stein, L. Evans, P. D. Calarco, and M. Kirschner. 1994. Pericentrin, a highly conserved centrosome protein involved in microtubule organisation. *Cell.* 76:639–650.

Egel, R. 1971. Physiological aspects of conjugation in fission yeast. *Planta.* 98:89–96.

Funabiki, H., I. Hagan, S. Uzawa, and M. Yanagida. 1993. Cell cycle–dependent specific positioning and clustering of centromeres and telomeres in fission yeast. *J. Cell Biol.* 121:961–976.

Goldstein, L. S. B. 1993. With apologies to Scheherazade: tails of 1001 kinesin motors. *Annu. Rev. Genet.* 27:319–351.

Gotoh, Y., E. Nishida, S. Matsuda, N. Shiina, H. Kosako, K. Shiokawa, T. Akiyama, K. Ohta, and H. Sakai. 1991. In vitro effects on microtubule dynamics of purified Xenopus M phase-activated MAP kinase. *Nature (Lond.).* 349:251–254.

Grimm, C., J. Kholi, J. Murray, and K. Maundrell. 1988. Genetic engineering of *Schizosaccharomyces pombe*: a system for gene disruption and replacement using the ura4 gene as a selectable marker. *Mol. Gen. Genet.* 215: 81–86.

Gutz, H., H. Heslot, U. Leupold, and N. Loprieno. 1974. *In* Handbook of Genetics. R. C. King, editor. Plenum Press, NY. 395–445.

Hagan, I. M., and J. S. Hyams. 1988. The use of cell division cycle mutants to investigate the control of microtubule distribution in the fission yeast *Schizosaccharomyces pombe*. *J. Cell Sci.* 89:343–357.

Hagan, I., and M. Yanagida. 1990. Novel potential mitotic motor protein encoded by the fission yeast *cut7*$^+$ gene. *Nature (Lond.).* 347:563–566.

Hagan, I., and M. Yanagida. 1992. Kinesin related cut7 protein associates with mitotic and meiotic spindles in fission yeast. *Nature (Lond.).* 356:74–76.

Hagan, I., J. Hayles, and P. Nurse. 1988. Cloning and sequencing of the cyclin related *cdc13*$^+$ gene and a cytological investigation of its role in fission yeast mitosis. *J. Cell Sci.* 91:587–595.

Harlow, E., and D. Lane. 1988. Antibodies a Laboratory Manual. Cold Spring Harbor Laboratory Press, Cold Spring Harbor, NY. 53–319.

Hirano, T., Y. Hiraoka, and M. Yanagida. 1988. A temperature sensitive mutation of the *Schizosaccharomyces pombe*: gene *nuc2+* that encodes a nuclear scaffold-like protein blocks spindle elongation in mitotic anaphase. *J. Cell Biol.* 106:1171–1183.

Hirano, T., N. Kinoshita, K. Morikawa, and M. Yanagida. 1990. Snap helix with knob and hole: essential repeats in *S. pombe* nuclear protein *nuc2*$^+$. *Cell.* 60:319–328.

Hirano, T., S. Funahashi, T. Uemura, and M. Yanagida. 1986. Isolation and characterisation of *Schizosaccharomyces pombe* cut mutants that block nuclear division but not cytokinesis. *EMBO (Eur. Mol. Biol. Organ.) J.* 5:2973–2979.

Hirata, A., and K. Tanaka. 1982. Nuclear behaviour during conjugation and meiosis in the fission yeast *Schizosaccharomyces pombe*. *J. Gen. Appl. Microbiol.* 28:263–274.

Hirata, A., and C. Shimoda. 1994. Structural modification of spindle pole bodies during meiosis II is essential for the normal formation of the ascospores in *Schizosaccharomyces pombe*: ultrastructural analysis of spo mutants. *Yeast.* 10:173–183.

Horio, T., S. Uzawa, M. K. Jung, B. R. Oakley, K. Tanaka, and M. Yanagida. 1991. The fission yeast γ-tubulin is essential for mitosis and is localized at microtubule organising centres. *J. Cell Sci.* 99:693–700.

Hoyt, M., L. He, K. Loo, and W. Saunders. 1992. Two *Saccharomyces cerevisiae* kinesin-related gene products required for mitotic spindle assembly. *J. Cell Biol.* 1189:109–120.

Masuda, H., T. Hirano, M. Yanagida, and W. Z. Cande. 1990. In vitro reactivation of spindle elongation in fission yeast nuc2 mutant cells. *J. Cell Biol.* 110:417–425.

Masuda, H., M. Sevik, and W. Z. Cande. 1992. *In vitro* microtubule nucleating activity of spindle pole bodies in fission yeast *Schizosaccharomyces pombe*: cell cycle-dependent activation in *Xenopus* cell-free extracts. *J. Cell Biol.* 117:1055–1066.

Maundrell. 1990. *nmt1*$^+$ of fission yeast. *J. Biol. Chem.* 265:10857–10864.

Maundrell, K. 1993. Thiamine-repressible expression vectors pREP and pRIP for fission yeast. *Gene (Amst.).* 123:127–130.

McCully, K., and C. F. Robinow. 1971. Mitosis in the fission yeast *Schizosaccharomyces pombe*: a comparative study with light and electron microscopy. *J. Cell Sci.* 9:475–507.

McNally, F. J., and R. D. Vale. 1993. Identification of katanin, an ATPase that severs and disassembles stable microtubules. *Cell.* 75:419–429.

Moreno, S., A. Klar, and P. Nurse. 1990. An introduction to molecular analysis of the fission yeast *Schizosaccharomyces pombe*. *Methods Enzymol.* 194: 793–823.

Nilsson, T., M. H. Hoe, P. Slusarewicz, C. Rabouille, R. Watson, F. Hunte, G. Watzele, E. C. Berger, and G. Warren. 1994. Kin recognition between *medial* Golgi enzymes in HeLa cells. *EMBO (Eur. Mol. Biol. Organ.) J.* 13:562–564.

Nurse, P. 1990. Universal control mechanism regulating onset of M-phase. *Nature (Lond.).* 344:503–508.

Oakley, C., and B. Oakley. 1989. Identification of γ-tubulin, a new member of the tubulin superfamily encoded by mipA gene of *Aspergillus nidulans*. *Nature (Lond.).* 338:662–664.

Page, B. D., L. L. Satterwhire, M. Rose, and M. Snyder. 1994. Localization of Kar3 kinesin heavy chain-related protein requires the cik1 interacting protein. *J. Cell Biol.* 124:507–519.

Rieder, C. L., and E. D. Salmon. 1994. Motile kinetochores and polar ejection forces dictate chromosome position on the vertebrate spindle. *J. Cell Biol.* 124:223–233.

Robinow, C. F. 1977. The number of chromosomes in *Schizosaccharomyces pombe*: light microscopy of stained preparations. *Genetics.* 87:491–497.

Rose, M. D., and G. R. Fink. 1987. KAR1, a gene required for function of both intranuclear and extranuclear microtubules in yeast. *Cell.* 48:1047–

1060.
Sambrook, J., E. F. Fritsch, and T. Maniatis. 1989. Molecular Cloning. Cold Spring Harbor Laboratory Press, Cold Spring Harbor, New York. 1.1–I47.
Samejima, I., T. Matsumoto, Y. Nakaseko, D. Beach, and M. Yanagida. 1993. Identification of seven new *cut* genes involved in *Schizosaccharomyces pombe* mitosis. *J. Cell Sci.* 105:135–143.
Samejima, I., and M. Yanagida. 1994. Bypassing anaphase by fission yeast cut9 mutation: requirement of *cut9*$^{+}$ to initiate anaphase. *J. Cell Biol.* 127: 1655–1671.
Saunders, W. S., and M. A. Hoyt. 1992. Kinesin related proteins required for structural integrity of the mitotic spindle. *Cell.* 70:451–458.
Shiina, N., Y. Gotoh, and E. Nishida. 1992. A novel homo-oligomeric protein responsible for an MPF-dependent microtubule severing activity. *EMBO (Eur. Mol. Biol. Organ.) J.* 11:4723–4731.
Studier, F. W., A. H. Rosenburg, J. J. Dunn, and J. W. Dubenhoff. 1990. Use of T7 RNA polymerase to direct expression of cloned genes. *Methods Enzymol.* 185:60–89.
Tanaka, K., and A. Hirata. 1982. Ascospore development in the fission yeast *Schizosaccharomyces pombe*. *J. Cell Sci.* 56:263–279.
Tanaka, K., and T. Kanbe. 1986. Mitosis in the fission yeast *Schizosaccharomyces pombe* as revealed by freeze-substitution electron microscopy. *J. Cell Sci.* 80:253–268.
Thomas, J., and D. Botstein. 1986. A gene required for the separation of chromosomes on the spindle apparatus in yeast. *Cell.* 44:65–76.
Vale, R. D. 1991. Severing of stable microtubules by mitotically activated protein in Xenopus egg extracts. *Cell.* 64:827–839.
Vallen, E. A., M. A. Hiller, T. Y. Scherson, and M. D. Rose. 1992*a*. Separate domains of *KAR1* mediate distinct functions in mitosis and nuclear fusion. *J. Cell Biol.* 117:1277–1287.
Vallen, E. A., T. Y. Scherson, T. Roberts, K. vanZee, and M. D. Rose. 1992*b*. Asymetric mitotic segregation of the yeast spindle pole. *Cell.* 69:505–515.
Verde, F., J.-C. Labbe, M. Doree, and E. Karsenti. 1990. Regulation of microtubule dynamics by cdc2 protein kinase in cell-free extracts of *Xenopus* eggs. *Nature (Lond.).* 343:233–238.
Verde, F., M. Dogterom, E. Steuzer, and E. Karsenti. 1992. Control of microtubule dynamics and length by cyclin A- and cyclin B-dependent kinases in *Xenopus*. *J. Cell Biol.* 118:1109–1108.
Winey, M., L. Goetsch, P. Baum, and B. Byers. 1991. *MPS1* and *MPS2*: novel genes defining distinct steps of spindle pole body duplication. *J. Cell Biol.* 114:745–754.
Winey, M. L., M. A. Hoyt, C. Chan, L. Goetsch, D. Botstein, and B. Byers. 1993. NDC1: a nuclear periphery component required for yeast spindle pole body duplication. *J. Cell Biol.* 122:743–751.
Woods, A., T. Sherwin, R. Sasse, T. H. MacRae, A. J. Baines, and K. Gull. 1989. Definition of individual components within the cytoskeleton of *Trypanosoma brucei* by a library of monoclonal antibodies. *J. Cell Sci.* 93: 491–500.
Yanagida, M. 1987. Yeast tubulin genes. *Microbiol. Sci.* 4:115–118.
Yanagida, M. 1989. Gene products required for chromosome separation. *J. Cell Sci. Suppl.* 12:213–229.